Interaction of Gold Nanoparticle with Human Serum Albumin (HSA) Protein Using Surface Energy Transfer

ARTICLE *in* THE JOURNAL OF PHYSICAL CHEMISTRY C · SEPTEMBER 2011

Impact Factor: 4.77 · DOI: 10.1021/jp207374g

5 AUTHORS, INCLUDING:

Shubhasis Haldar
University of California
11 PUBLICATIONS **101** CITATIONS
SEE PROFILE

Krishnananda Chattopadhyay
Indian Institute of Chemical Biology
40 PUBLICATIONS **906** CITATIONS
SEE PROFILE

Amitava Patra
Indian Association for the Cultivation of Scie…
172 PUBLICATIONS **4,129** CITATIONS
SEE PROFILE

THE JOURNAL OF PHYSICAL CHEMISTRY C

ARTICLE

pubs.acs.org/JPCC

Interaction of Gold Nanoparticle with Human Serum Albumin (HSA) Protein Using Surface Energy Transfer

Tapasi Sen,[†] Sadananda Mandal,[†] Shubhasis Haldar,[‡] Krishnananda Chattopadhyay,[‡] and Amitava Patra*[,†]

[†]Department of Materials Science, Indian Association for the Cultivation of Science, Kolkata 700 032, India

[‡]Structural Biology and Bioinformatics Division, Indian Institute of Chemical Biology, Council of Scientific and Industrial Research, Kolkata 700 032, India

Supporting Information

ABSTRACT: Here, we study the human serum albumin (HSA) protein−Au nanoparticle interaction to identify the specific binding site of protein with nanoparticles by using the surface energy transfer (SET) method among tryptophan (Trp) of HSA, ANS-dye-labeled HSA protein, and Au nanoparticles. Here, ANS dye is used as a probe located at domain IIIA of HSA. In particular, absorbance, fluorescence quenching, decay time, circular dichroism, dynamic light scattering, and TEM measurements are performed to understand the physical properties of protein-conjugated Au nanoparticles. Using the SET method, the measured distances between the Trp residue of HSA and the binding site of HSA interacting with Au nanoparticles are 42.5, 41.9, and 48.1 Å for 1.5, 2.0, and 2.9 nm HSA-conjugated Au nanoparticles, respectively. The measured distances between the binding site of ANS dye (located at domain IIIA) in HSA to the binding site of HSA interacting with Au nanoparticles are 51, 51.5, and 54.7 Å for 1.5, 2.0, and 2.9 nm HSA-conjugated Au nanoparticles, respectively. From the protein structural data (using PyMol software), the distances from the center of domain IIIA to Cys53−Cys62 disulfide bond and Trp to Cys53−Cys62 disulfide bond are obtained to be 51.5 and 39.1 Å, respectively. Thus, the distances calculated by using SET equation (Trp to Au binding site distance and ANS to Au binding site distance) nicely match with the distances obtained from protein structural data by using PyMol software. Analysis suggests that the Au nanoparticle is attached to HSA by linkage through Cys53−Cys62 disulfide bond which is located at subdomain IA of HSA.

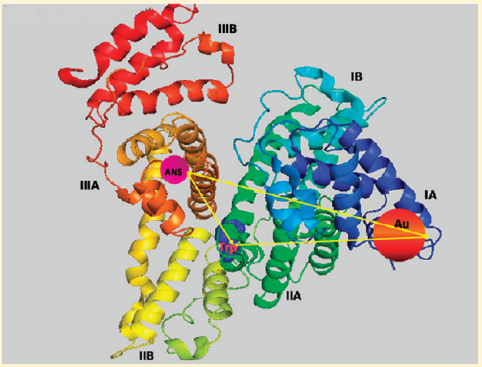

INTRODUCTION

Research in bioconjugated nanoparticles has been paid great attention because of their promising applications such as luminescence tagging, imaging, medical diagnostics, multiplexing, and most recently biosensors.[1−6] Despite the remarkable advancement of nanoscience, relatively little is known about the effects of nanoscale objects on biological systems and their potential toxicity.[7] The understanding of the interaction of proteins with nanoparticles is still of great concern for their successful use in nanomedicine and nanotoxicology.[7−10] During the interactions of nanoparticles with proteins, that may alter protein conformation, expose novel epitopes on the protein surface, or perturb the normal protein function, which could induce unexpected biological reactions and lead to toxicity.[7,8]

Human serum albumin (HSA)[11,12] is the most abundant protein in plasma, present at a concentration of ∼0.6 mM. The functions of HSA include the maintenance of colloid osmotic pressure and transportation and metabolism of many endogenous and exogenous ligands (i.e., fatty acids, hormones, several metals). HSA, a globular protein of M_r 66 kDa, consists of 585 amino acids. Its amino acid sequence contains 18 tyrosines, 6 methionines, 1 tryptophan (Trp 214), 17 disulfide bridges, and only one free thiol (Cys 34). The disulfides are positioned in a repeating series of nine loop−link−loop structures centered on eight sequential Cys-Cys pairs. HSA comprises three homologous domains (I, II, and III) that assemble to form a heart-shaped molecule. Each domain contains two subdomains (A and B) that possess common structural motifs.[11,13] The main regions of ligand interaction are located in hydrophobic pockets at subdomains IIA and IIIA, IIIA having the highest affinity.[11] Many ligands bind specifically to HSA, either in site I (located at subdomain IIA) or in site II (located at subdomain IIIA).[13] The binding of the ligands with active sites of the proteins can change their structure and function and cause toxic effects.[14] The single tryptophan of HSA at residue 214 has been used extensively as a fluorescent reporter group for ligand binding and conformational studies.[15,16] Fluorescent probes are of great aid in the study of interactions between drugs and serum albumins and in revealing fine features of structure and dynamics.[13] The fluorescent probe 1-anilino-8-naphthalenesulfonate (ANS) is being

Received: August 2, 2011
Revised: November 1, 2011
Published: November 03, 2011

used in many studies to monitor the binding sites of serum albumins, and the binding of this fluorophore to HSA has been well characterized.[17] ANS dye has been defined as a site II (subdomain IIIA) probe.[13,17]

Recently, gold nanoparticles have been used as a model[18] for understanding nanoparticle−protein interactions because of their promise for diverse biomedical applications, including their use as probes in many biodiagnostic systems, and photothermal and targeted drug delivery treatments of cancer.[19] The choice also fell on gold nanoparticles because they are inert, and they possesses facile bioconjugation ability, which is desired for quantitative analyses.[20] Recently, Douglas et al.[18] reported the interaction of gold nanoparticles of different sizes with common blood proteins: albumin, fibrinogen, γ-globulin, histone, and insulin. They found that gold NPs strongly associate with these essential blood proteins where the binding constant depends on particle size and the native protein structure, and the model proteins undergo conformational change upon association with the NPs. In most of the studies, the information about protein structural changes upon binding to nanoparticles and the identification of the protein binding site has been based mainly on infrared spectroscopy, circular dichroism, fluorescence, and other methods that can monitor changes in the secondary and tertiary structure of proteins.[21] However, these techniques give limited information at the amino acid level. NMR study is also a well-established technique used to monitor protein−protein interaction and protein−ligand interactions.[22a] Rossi et al.[22a] reported the interaction of human ubiquitin (hUbq) with gold nanoparticles and identifies the specific protein domain that interacts with AuNP using NMR. However, the major drawback of the NMR technique lies on the limitation of size of proteins that can be measured.[22a]

Our motivation is to study the HSA protein−Au nanoparticle interaction using steady-state and time-resolved spectroscopy to identify the specific binding site of protein with nanoparticles by using surface energy transfer among tryptophan of HSA, ANS-dye-labeled HSA protein, and Au nanoparticles. For this purpose, we have prepared HSA-conjugated Au nanoparticles of three different sizes, and ANS dye is labeled as a probe in these bioconjugated Au nanoparticles systems. It is known that ANS dye is located in the hydrophobic pocket of subdomain IIIA of HSA.[13]

Förster resonance energy transfer (FRET) is widely used to measure the distance between a donor and an acceptor. FRET occurs through the dipole−dipole interactions between an excited donor (D) molecule and an acceptor (A) and the efficiency of FRET depends on the inverse sixth power of the distance of separation (d^{-6}) between donor and acceptor.[23,24] However, the FRET process is restricted by its upper limit of separation of only 80 Å. Recently, the surface energy transfer (SET) between Au nanoparticle and dye provides a new paradigm to design an optical-based molecular ruler for long distance measurement. SET is originated from the interaction of the electromagnetic field of the donor dipole with the free conduction electrons of the accepting metal. The mechanism of dye quenching at Au nanoparticle surface is already demonstrated and it is found that the separation between donor and acceptor is d^{-4} dependent.[23−28] Thus, the surface energy transfer is being used to understand the specific binding site of HSA with Au nanoparticles. Again, we try to understand whether the conformation of HSA protein changes upon conjugation with different sized Au nanoparticles.

EXPERIMENTAL METHODS

Reagents. Chloroauric acid ($HAuCl_4 \cdot 3H_2O$) (Loba Chemei), sodium borohydride ($NaBH_4$) (Merck), human serum albumin (HSA) (Sigma), and 8-anilino-1-naphthalenesulfonic acid (ANS dye) (Aldrich) were used without further purification.

Synthesis of Three Different-Sized HSA-Conjugated Au Nanoparticles. HSA-conjugated Au nanoparticles of different sizes at pH 7.0 were synthesized using our previously reported method.[26] For the preparation of three different-sized HSA-conjugated Au nanoparticles, 0.007 g of HSA was dissolved in 9.5 mL of 10 mM PBS buffer solution at pH 7.0 in three different beakers, and marked as A, B, and C. Then 0.5, 0.25, and 0.125 mL of 10 mM $HAuCl_4$ solution were added to A, B, and C, respectively. The total volume of each solution was 10 mL. After 5 min of stirring, 70, 50, and 20 μL of ice cold $NaBH_4$ aqueous solution (0.001 g/mL) were added to A, B and C, respectively, under mild stirring condition. The color of the solutions changes from light yellow to reddish brown. This indicates the formation of Au nanoparticles. All the colloidal solutions were stored at 4 °C prior to use. For the incorporation of ANS dye in HSA, 0.3 mL of 90 μM ANS solution was added to 2.7 mL of each of the colloidal HSA-conjugated Au solutions. All the solutions were kept for 24 h for stabilization. After 1 day, dye-containing HSA-conjugated Au nanoparticles solutions were used for optical study.

The transmission electron microscopy (TEM) images were taken using a JEOL-TEM-2010 transmission electron microscope with an operating voltage of 200 kV. Room-temperature optical absorption spectra were obtained with an UV−vis spectrophotometer (Shimadzu). CD spectra were taken on a JASCO J-815 CD spectrometer (J-815-150S) with a rectangular quartz cell having 1.0 mm path length. All CD spectra were taken in a wavelength range of 200−250 nm, and each spectrum was the accumulation of three scans. The emission spectra of all samples were recorded in a Fluoro Max-P (Horiba Jobin Yvon) luminescence spectrophotometer. For the time-correlated single-photon-counting (TCSPC) measurements, the samples were excited at 280 nm using a light-emitting diode and 375 nm using a picosecond diode laser in an IBH Fluorocube apparatus. The typical fwhm of the system responses for 280 nm LED and 375 nm diode laser using a liquid scatter are about 1.24 ns and 300 ps, respectively. The repetition rate is 1 MHz. The fluorescence decays were collected on a Hamamatsu MCP photomultiplier (C487802). The fluorescence decays were analyzed using IBH DAS6 software. The following expression was used to analyze the experimental time-resolved fluorescence decays, $I(t)$:

$$I(t) = \sum_{i=1}^{n} \alpha_i \exp(-t/\tau_i) \quad (1)$$

Here, n is the number of discrete decay components, and α_i and τ_i are the pre-exponential factors and excited-state fluorescence lifetimes associated with the ith component, respectively.[29]

For anisotropy measurements, a polarizer was placed before the sample. The analyzer was rotated by 90° at regular intervals and the parallel ($I_\parallel$) and perpendicular ($I_\perp$) components for the fluorescence decay were collected for equal times, alternatively. Then, $r(t)$ was calculated using the formula[29]

$$r(t) = \frac{I_\parallel(t) - GI_\perp(t)}{I_\parallel(t) + 2GI_\perp(t)} \quad (2)$$

The G value of the setup is 0.70.

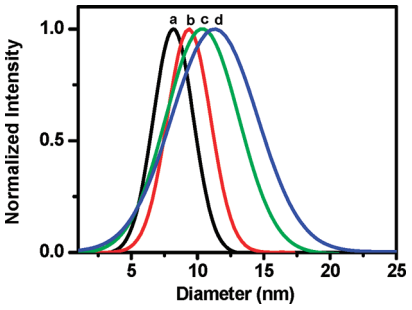

Figure 1. DLS spectra of pure HSA (curve a), 1.5 nm sized Au-HSA (curve b), 2.0 nm sized Au-HSA (curve c), and 2.9 nm sized Au-HSA (curve d).

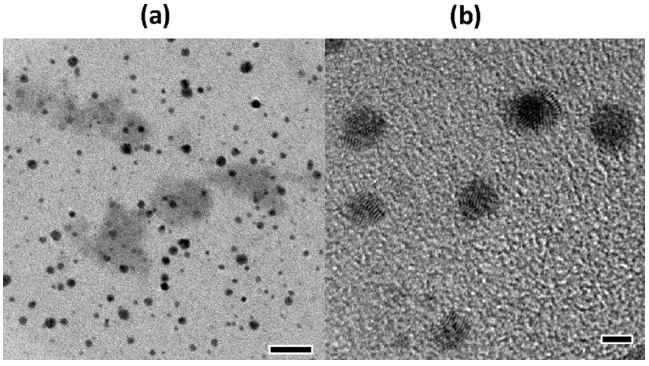

Figure 2. (a) TEM images of HSA-conjugated Au nanoparticles of 2.9 nm size (scale bar = 20 nm), and (b) the corresponding HRTEM images (scale bar = 2 nm).

MALDI mass spectrometry was performed using a 4800 MALDI-TOF-TOF mass spectrometer (Applied Biosystems, USA) equipped with a gridless ion source delayed extraction and the instrument was operated in linear mode. The delay time of 500 ns was used, and the spectra were acquired by averaging 600−800 shots.

For the reverse-phase HPLC separation, 0.7 mg of HSA tagged with gold nanoparticle was dissolved in 1 mL of 50 mM sodium phosphate buffer pH 7. Reverse-phase HPLC separations were performed by a μBondapak C18 column (250 × 4 mm, 5 μm particle size) using a HPLC system (Waters, Singapore). A linear gradient of 0.1% TFA in water and acetonitrile with a flow rate of 1.2 mL/min was used for 60 min for the elution purpose.

RESULTS AND DISCUSSION

Dynamic Light Scattering (DLS) and Transmission Electron Microscopy (TEM) Studies. Dynamic light scattering (DLS) measurement of pure HSA at pH 7.0 (shown in Figure 1) reveals the hydrodynamic diameter of 8.0 nm, which exactly matches the reported hydrodynamic diameter of HSA protein (8.0 nm) at pH 7.4.[30] DLS spectra of HSA-conjugated Au nanoparticles of different sizes (Figure 1) show monodisperse particle size distribution with hydrodynamic diameters of 9.4, 10.2, and 11.2 nm. Thus, the hydrodynamic diameter increases from HSA to Au-HSA, and the increments are 1.4, 2.2, and 3.2 nm. These increments nicely match with the average sizes of the HSA-conjugated Au nanoparticles obtained from TEM images of Au nanoparticles which are 1.5, 2.0, and 2.9 nm sized Au-HSA at pH 7.0, respectively (shown in Figure 2 and Figure S1 in the Supporting Information). It reveals that the Au nanoparticle is strongly interacting with HSA protein and the ratio of HSA and Au nanoparticles in the HSA−Au conjugates is 1:1.[22]

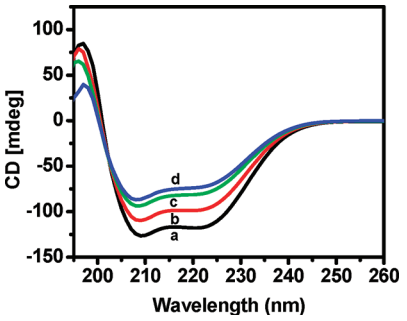

Figure 3. CD spectra of pure HSA (curve a), 1.5 nm sized Au-HSA (curve b), 2.0 nm sized Au-HSA (curve c), and 2.9 nm sized Au-HSA (curve d).

Circular Dichroism (CD) Study. CD spectroscopy is one of the most commonly used methods to study the protein conformations in solution. Figure 3 shows the far-UV CD spectra of native HSA and three different-sized Au-conjugated HSA solutions. The CD spectrum of HSA at pH 7.0 exhibits two negative minima in the ultraviolet region at 208 and 222 nm, which are the characteristics of an α-helical structure of the protein.[26] We can see from the spectra that the ellipticity of HSA decreases after conjugation with Au nanoparticles, which indicates that some kind of partial unfolding of HSA is occurring upon conjugation with Au nanoparticles. The percentages of α-helicity of pure HSA- and Au-conjugated HSA are calculated from the mean molar residual ellipticity (θ_{MRE}) values.[31] Thus the loss of α-helical content of HSA protein are found to be 9, 18, and 22% for 1.5, 2.0, and 2.9 nm sized Au nanoparticles conjugated HSA, respectively. It reveals that the extent of unfolding of HSA increases with increasing the size of the Au nanoparticles.

MALDI Mass Spectrometry and Reverse Phase HPLC Separation. To reveal quantitative estimation on protein−nanoparticle interactions, reversed phase chromatographic elution profiles of protein before and after conjugation with nanoparticle is necessary.[7] Elution of the HSA-conjugated Au nanoparticle (2.9 nm size) was monitored using a dual-wavelength UV−vis detector at 280 and 526 nm, respectively (shown in Supporting Information, Figure S2). The peak centered at 280 nm is characteristic of protein absorbance whereas peak at 526 nm arises due to the Au nanoparticles. The HPLC elution profile shows a single peak at the retention time of 43 min observed by both detectors (at 280 nm and at 526 nm). Elution of HSA together with Au nanoparticles with the same retention time indicates that all HSA proteins are tagged with Au nanoparticles and no free HSA is left in the solution.

Steady-State and Time-Resolved Study. Figure 4A shows the absorption spectra of native HSA in phosphate buffer (pH 7.0) and HSA-conjugated with different sizes of Au nanoparticles. As shown in curve a (Figure 4A), pure HSA exhibits an absorption maximum at 278 nm, which originates from the aromatic residues tryptophan, tyrosine and the disulfide bonds in the protein.[32] Surface plasmon bands at 526 and 520 nm are obtained for 2.9 and 2.0 nm HSA-conjugated Au nanoparticles, respectively. The absorption peak is not expected for 1.5 nm Au nanoparticles due to very small particle size.[23]

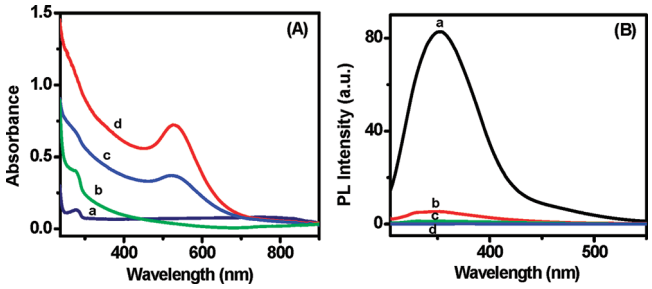

Figure 4. (A) Absorption spectra of pure HSA (curve a), 1.5 nm sized Au-HSA (curve b), 2.0 nm sized Au-HSA (curve c), and 2.9 nm sized Au-HSA (curve d). (B) Emission spectra of pure HSA (curve a), 1.5 nm sized Au-HSA (curve b), 2.0 nm sized Au-HSA (curve c), and 2.9 nm sized Au-HSA (curve d) (λ_{ex} = 295 nm).

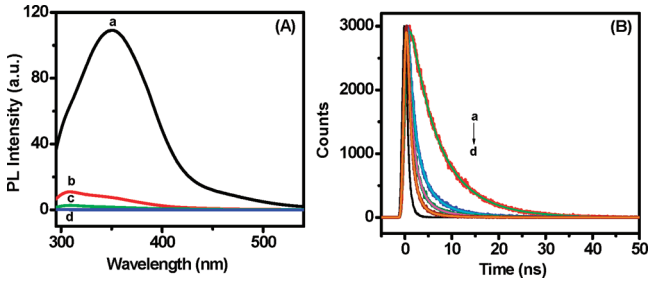

Figure 5. (A) Emission spectra of pure HSA (curve a), 1.5 nm sized Au-HSA (curve b), 2.0 nm sized Au-HSA (curve c), and 2.9 nm sized Au-HSA (curve d) (λ_{ex} = 280 nm). (B) Corresponding time-resolved spectra of pure HSA (curve a), 1.5 nm sized Au-HSA (curve b), 2.0 nm sized Au-HSA (curve c), and 2.9 nm sized Au-HSA (curve d) (λ_{ex} = 280 nm).

To gain more specific local information about the binding of nanoparticle to protein, the fluorescence measurement of the tryptophan (Trp) residue of the protein is widely applied because of the high sensitivity of tryptophan emission to the local environment.[18] HSA possesses one Trp residue residing on the bottom of hydrophobic pocket in domain IIA (Trp-214). The effect of Au nanoparticles on the photoluminescence intensity of Trp of HSA upon excitation at 295 nm is illustrated in Figure 4B. Excitation wavelength of 295 nm is used to avoid the contribution from the tyrosine and phenylalanine residues present in HSA. From the emission spectra, it is clear that the tryptophan fluorescence (curve a) is drastically quenched in the presence of Au nanoparticles (curves b−d). The observed PL quenching efficiencies are 93.4%, 98.5%, and 99.9% for 1.5, 2.0, and 2.9 nm Au nanoparticles conjugated HSA, respectively. Such strong quenching implies that Au nanoparticle binds to HSA at a location near the Trp residue in all three conjugated systems. It is interesting to note that the size of nanoparticles influence the PL quenching efficiency of Trp. The samples are also excited at 280 nm to determine the effect of Au nanoparticles on the overall PL intensity of the protein and the corresponding emission spectra are shown in Figure 5A. The emission at 350 nm is due to tryptophan residue of HSA. The observed PL quenching efficiencies are 93.1%, 98.4%, and 99.9% for 1.5, 2.0, and 2.9 nm Au nanoparticles conjugated HSA, respectively (considering emission intensity at 350 nm). This result is identical with the observed PL quenching efficiencies of Trp upon excitation at 295 nm. Figure 5B shows the time-resolved fluorescence spectra of pure HSA and HSA-conjugated with different sizes of Au nanoparticles upon excitation at 280 nm LED monitoring the emission wavelength at 350 nm. The photoluminescence decays of tryptophan in pure HSA protein and in HSA-conjugated different sizes of Au nanoparticle solutions are fitted to triexponential functions. For pure HSA protein, three lifetime components of 0.269 ns (19%), 4.13 ns (34%), and 7.81 ns (47%) are observed (listed in Table 1). This result nicely matches with the previous reports on the time-resolved fluorescence lifetime measurements of tryptophan in HSA.[33−37] Albani et al.[33] reported the three-exponential decay of Trp residue in HSA protein in the absence and presence of quencher. They obtained the decay times of 0.528, 3.566, and 7.460 ns with the pre-exponential factors of 0.1235, 0.3104, and 0.5661 for Trp in HSA. Rolinski et al.[34] reported three-exponential decays of HSA, for both with quercetin and without quercetin. They found three lifetimes of 0.793 ns (0.0205), 4.089 ns (0.4459), and 7.145 ns (0.5335) for free HSA. Our result is also in consistent with measurements reported by Amiri et al.,[35] Flora et al.,[36] and Zolese et al.[37] Recent studies have shown that the two shortest lifetimes around 0.4−0.5 and 2−4 ns were measured for tryptophan free in solution and present within proteins.[38] These two lifetimes are independent of any structure around tryptophan and characterize an internal property or/and organization of the tryptophan structure in the excited state.[38] The presence of third lifetime could be attributed to interaction between the Trp residue (s) and the surrounding amino acids and to possible specific properties of the protein.[38] In the present study, the average lifetime ($\langle\tau\rangle$) of Trp is found to be 5.13 ns. In the presence of different-sized Au nanoparticles, the lifetime of Trp is also three exponential. The observed average decay times are 1.37, 0.685, and 0.413 ns for 1.5, 2, and 2.9 nm Au-conjugated HSA, respectively (Table 1). It clearly reveals that there is a shortening of the decay time of tryptophan in presence of Au nanoparticles, confirming the energy transfer occurs from tryptophan to Au nanoparticles. Rolinski et al.[34] reported the decrease in lifetime of HSA in the presence of quercetin that indicates energy transfer from Trp to quercetin. In the present study, the calculated energy-transfer efficiencies from tryptophan to Au nanoparticles are 73%, 87%, and 92%, for 1.5 nm Au-conjugated HSA, 2 nm Au-conjugated HSA, and 2.9 nm Au-conjugated HSA, respectively (Table 1). The lifetime data also implies that the energy-transfer efficiency of tryptophan increases with increase in the size of the Au nanoparticles. Analysis suggests that the energy transfer depends on the size of nanoparticles.

In this study, the distance between donor (tryptophan) and acceptor (Au nanoparticle) has been calculated by using the surface energy transfer (SET) method. The characteristic distance d_0 value is calculated using the Persson model[23−28]

$$d_0 = \left(\frac{0.225c^3\Phi_d}{\omega_d^2\omega_F k_F}\right)^{1/4} \quad (3)$$

where d_0 is the distance at which a donor will display equal probabilities for energy transfer and spontaneous emission. Φ_d is the quantum efficiency of tryptophan (0.118), ω the frequency of the donor electronic transition, ω_F the Fermi frequency, and k_F Fermi wave vector of the metal.[23,24] The d_0 value is calculated using Φ_{Trp} = 0.118, $\omega = 6.73 \times 10^{15}$ s^{-1}, $\omega_F = 8.4 \times 10^{15}$ s^{-1}, and $k_F = 1.2 \times 10^8$ cm^{-1}, and $c = 3 \times 10^{10}$ cm s^{-1}. The calculated d_0 value is 35.2 Å for HSA-conjugated Au nanoparticles. The

Table 1. Fluoresence Decay Parameters of Tryptophan of HSA in the Absence and Presence of Au Nanoparticles (λ_{em} = 350 nm)

system	a_1	τ_1 (ns)[a]	a_2	τ_2 (ns)[a]	a_3	τ_3 (ns)[a]	$\langle\tau\rangle$ (ns)[a]	ϕ_{ET} (%)	d (Å)
pure HSA at pH 7	0.19	0.269	0.34	4.13	0.47	7.81	5.13	–	–
Au(1.5 nm)-HSA at pH 7	0.66	0.507	0.25	2.04	0.09	5.79	1.37	73	27.5
Au(2.0 nm)-HSA at pH 7	0.77	0.315	0.20	1.45	0.03	5.06	0.685	87	21.9
Au(2.9 nm)-HSA at pH 7	0.88	0.265	0.11	1.25	0.01	4.20	0.413	92	19.1

[a] $a_i = (\alpha_i)/(\Sigma_i\alpha_i)$, $\langle\tau\rangle = \Sigma_{i=1}^{n} a_i\tau_i$, $[a] = \pm 5\%$.

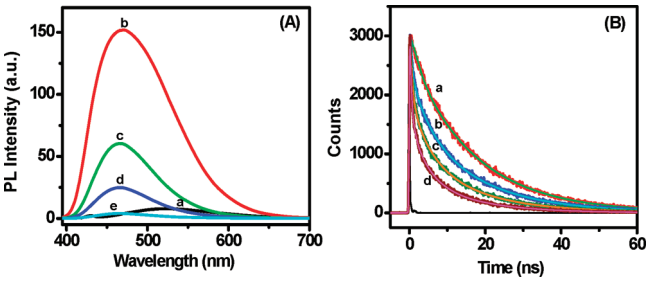

Figure 6. (A) Photoluminescence spectra of ANS dye in (a) water (b) pure HSA, (c) 1.5 nm Au nanoparticles conjugated HSA, (d) 2.0 nm Au nanoparticles conjugated HSA, and (e) 2.9 nm Au nanoparticles conjugated HSA (λ_{ex} = 375 nm). (B) Photoluminescence decay spectra of ANS dye in (a) pure HSA, (b) 1.5 nm Au nanoparticles conjugated HSA, (c) 2.0 nm Au nanoparticles conjugated HSA, and (d) 2.9 nm Au nanoparticles conjugated HSA (λ_{ex} = 375 nm).

quantum efficiency of energy transfer in surface energy transfer process can be written as[23,24]

$$\phi_{ET} = \frac{1}{1 + \left(\frac{d}{d_0}\right)^4} \quad (4)$$

The calculated distances (d) between the donor and acceptor are obtained to be 27.5, 21.9, and 19.1 Å for 1.5, 2.0, and 2.9 nm HSA-conjugated Au nanoparticles, respectively. It reveals that Au nanoparticles are situated at close proximity to the tryptophan residue for such quenching effect to occur. These distances are in consistent with the reported results.[26] Srinivasan et al.[39] found that the distance between Trp donor of HSA and bound piperine is 27.9 Å. Here, we found that the distance between Au nanoparticle and tryptophan decreases with increasing Au nanoparticle size. From this result, we may assume that Au nanoparticle may reside either in domain I or II or III of HSA because of the presence of thiolate (−SH) or disulfide (SS) linkage. To understand the exact location, i.e., the exact domain of HSA protein in which Au nanoparticle is being attached, we used three-body interactions where the binding positions of two moieties are fixed; the exact position of the third moiety has to be determined. For this purpose, ANS dye is used as a probe in this study, which is reported to bind in the active site of HSA protein in the subdomain IIIA.[13,17] Figure 6A shows the photoluminescence spectra of ANS dye in water and in HSA protein without and with conjugation with Au nanoparticles of different sizes. ANS dye being a hydrophobic dye does not show any fluorescence in water (curve a in Figure 6A). The emission spectrum (curve b in Figure 6A) shows strong fluorescence property of ANS dye in HSA protein. It implies that ANS dye is located in one of the hydrophobic pockets of HSA protein through hydrophobic interactions. It is reported that the main and most active binding site on HSA is located in subdomain IIIA of the protein molecules.[13] The binding site is a hydrophobic pocket formed by the spatial combination of the nonpolar residues. To understand the rotational dynamics of ANS dye molecules inside HSA protein, time-resolved anisotropy study is performed. Fluorescence anisotropy decay study reveals the reorientation dynamics of the excited fluorophore which directly help to understand structural information. The anisotropy decay of ANS in pure HSA and in 2.9 nm Au nanoparticle conjugated HSA protein is shown in Figure S3 in the Supporting Information. In pure HSA, the anisotropy decay of ANS (monitored at 468 nm) is single exponential with time constant of 39.6 ns. This anisotropy data is consistent with the previous results.[40−42] Castellano et al.[40] obtained a single rotational relaxation time of 41 ns for Ru(II) complex labeled to HSA. Ferrar et al.[41] extracted an effective rotational correlation time of 40 ± 2 ns for erythrosine bound to HSA. Bhattacharyya et al.[42] also reported rotational correlation time >40 ns for ANS bound to BSA. In this present study, the fluorescence anisotropy decay of ANS in 2.9 nm Au nanoparticle conjugated HSA protein (monitored at 468 nm) exhibits also a single-exponential decay with correlation time constant of 62.9 ns. This correlation time is characteristic of ANS that is tightly bound inside the protein and as a result it exhibits overall rotational motions of the whole protein.[43] The increase in the correlation time of ANS bound to Au-conjugated HSA compared to pure HSA may be explained by considering the Stokes−Einstein equation,[43b,44] i.e., $\tau_{rot} = \eta V/k_B T$, where τ_{rot} is the rotational time constant, η is the viscosity of the medium, and V is the volume of the rotating complex. In the case of ANS bound to Au-conjugated HSA, the hydrodynamic volume of the whole rotating moiety becomes larger compared to ANS bound to pure HSA and thus the anisotropy of the whole protein is seen to decay slowly (Supporting Information, Figure S3). Very recently, Laptenok et al.[43c] also obtained slow anisotropy decays of WFF apoflavodoxin protein at low denaturant concentrations because of the rigidly fixed Trp residue (W74) within the interior of native apoflavodoxin compared to that within the unfolded protein and thus it exhibits the slower overall rotational movements of the whole protein.

It is interesting to note that a drastic quenching in PL intensity of ANS emission in the presence of HSA-conjugated Au nanoparticles is observed (curves c−e in Figure 6A). The observed PL quenching efficiencies are 60.4%, 83.7%, and 97.4% for 1.5, 2.0, and 2.9 nm of HSA-conjugated Au nanoparticles, respectively, indicating that the quenching efficiency increases with the increase of the size of the Au nanoparticles. Figure 6B shows the time-resolved fluorescence spectra of ANS dye in aqueous solution of HSA and in the presence of different-sized HSA-conjugated Au nanoparticles. The photoluminescence decay of ANS dye in aqueous solution of HSA protein is biexponential. However, the fluorescence decay spectra of ANS dye in the presence of different-sized HSA-conjugated Au nanoparticles are

Table 2. Fluoresence Decay Parameters of ANS Dye of HSA in the Absence and Presence of HSA-Conjugated Au Nanoparticles at pH 7.0 (λ_{em} = 468 nm)

system	a_1	τ_1 (ns)[a]	a_2	τ_2 (ns)[a]	a_3	τ_3 (ns)[a]	$\langle\tau\rangle$ (ns)[a]	ϕ_{ET} (%)	d (Å)
ANS in pure HSA	–	–	0.18	2.26	0.82	16.9	14.3	–	–
ANS in Au(1.5 nm)-HSA	0.43	0.454	0.20	5.13	0.37	17.3	7.62	47	35.9
ANS in Au(2.0 nm)-HSA	0.50	0.587	0.24	5.18	0.26	16.3	5.78	60	31.5
ANS in Au(2.9 nm)-HSA	0.64	0.440	0.21	4.11	0.15	14.2	3.28	77	25.7

[a] $a_i = (\alpha_i)/(\Sigma_i\alpha_i)$, $\langle\tau\rangle = \Sigma_{i=1}^{n} a_i\tau_i$, $[a] = \pm 5\%$.

fitted to triexponential equations. The average decay times are 14.3, 7.6, 5.78 and 3.28 ns for ANS in pure HSA, 1.5, 2.0, and 2.9 nm HSA-conjugated Au nanoparticles, respectively (Table 2). The shortening of the decay time of ANS dye in the presence of Au naoparticles again confirms the energy transfer from ANS dye to Au nanoparticles. The energy-transfer efficiency from ANS dye to Au nanoparticles is being calculated by using the relation[29] $\phi_{ET} = 1 - \tau_{DA}/\tau_D$, where τ_{DA} is the decay time of dye in presence Au nanoparticles and τ_D corresponds to the decay time of dye in absence of Au nanoparticles. The calculated energy-transfer efficiencies from dye to Au nanoparticles are 46.7%, 59.6% and 77.1% for 1.5, 2.0, and 2.9 nm HSA-conjugated Au nanoparticles, respectively (Table 2). This indicates again that the energy-transfer efficiency increases with increase in the size of the HSA-conjugated Au nanoparticles. The calculated d_0 value is 34.7 Å for ANS dye interacting with HSA-conjugated Au nanoparticles, using the quantum yield of ANS in HSA protein (ϕ_d) = 0.07. The calculated distances (d) between the donor ANS and acceptor Au nanoparticles are 35.9, 31.5, and 25.7 Å for 1.5, 2.0, and 2.9 nm HSA-conjugated Au nanoparticles, respectively, using SET equation (eq 4).

The preferable binding of Au nanoparticles to HSA protein may be either through free Cys 34 residue or through Cys−Cys disulfide (SS) linkage because Au−S bond formation is energetically favorable.[27] Using the SET method, the measured distances between the surfaces of the Au nanoparticles and Trp residue are obtained to be 27.5, 21.9, and 19.1 Å for 1.5, 2.0, and 2.9 nm HSA-conjugated Au nanoparticles, respectively. Therefore, the distances between Trp residue and Au binds HSA protein are 42.5, 41.9, and 48.1 Å (upon addition of diameters of the Au nanoparticles with the corresponding distances obtained from SET) for 1.5, 2.0, and 2.9 nm HSA-conjugated Au nanoparticles, respectively. From the structural data of HSA protein using PyMol software, the distances from Trp to free Cys 34 (domain I), Cys53−Cys62 SS bond (domain I), Cys316−Cys361 SS bond (domain II), Cys360−Cys369 SS bond (domain II), and Cys558−Cys567 SS bond (domain III) are 34.1, 39.1, 27.3, 29.0, and 53.1 Å, respectively (shown in Figure 7A,B). These distances are close to the distances between Trp residue and the binding site of HSA with Au nanoparticles, obtained from SET. Therefore, these sites would be the probable binding sites of HSA with Au nanoparticles. Now, it is already reported that ANS dye is located in the hydrophobic pocket of subdomain IIIA of HSA.[13] The distances from the ANS to Au nanoparticles' surface are obtained to be 35.9, 31.5, and 25.7 Å for 1.5, 2.0, and 2.9 nm HSA-conjugated Au nanoparticles, respectively. Therefore, the distances between ANS dye and the binding site of HSA protein that interacts with Au nanoparticles are 51, 51.5, and 54.7 Å for 1.5, 2.0, and 2.9 nm HSA-conjugated Au nanoparticles, respectively. From the protein structural data (using PyMol software), the distances from the center of

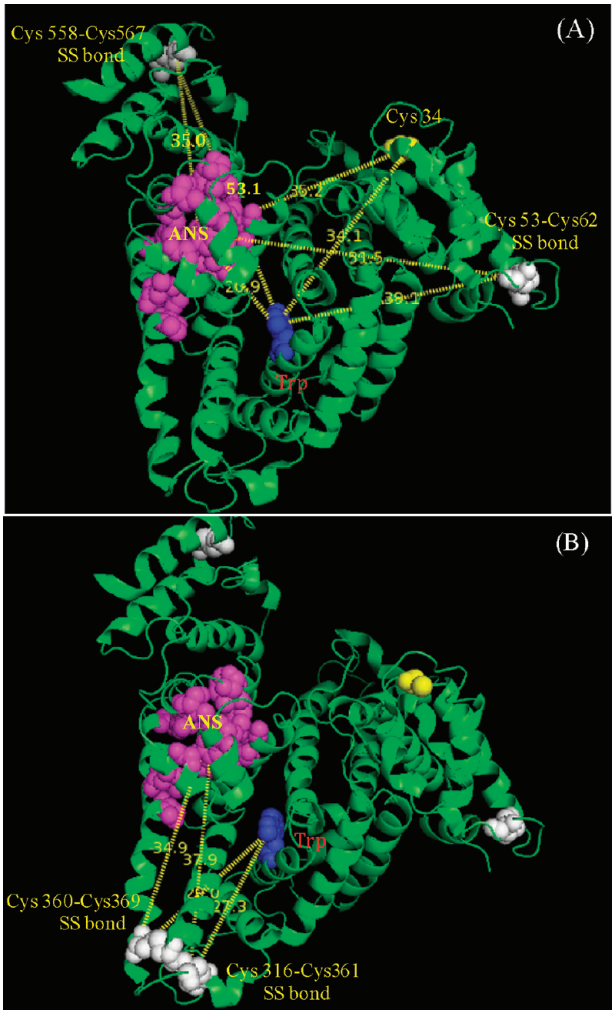

Figure 7. Schematic representations of different residues in HSA protein and their distances from tryptophan using Pymol software.

subdomain IIIA to Cys 34, Cys53−Cys62 SS bond (domain I), Cys316−Cys361 SS bond (domain II), Cys360−Cys369 SS bond (domain II), and Cys558−Cys567 SS bond (domain III) are found to be 35.2, 51.5, 37.9, 34.9, and 35.0 Å, respectively (shown in Figure 7). Thus all the conditions (Trp to Au binding site distance and ANS to Au binding site distance) would be satisfied only if Au nanoparticles bind to HSA through Cys53−Cys62 disulfide bond (subdomain IA).[11] The attachment of Au nanoparticles at this domain may be explained by considering the geometrical accommodation and the chemical environment of this domain in HSA. Domain IA is less hydrophobic and less sterically crowded compared to the more active binding sites

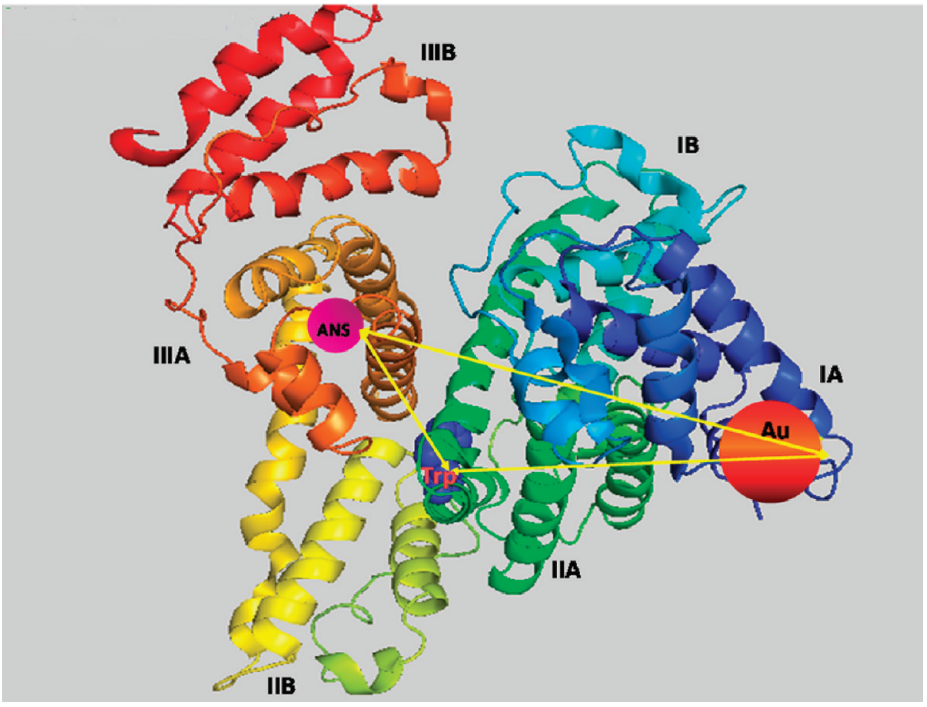

Figure 8. Schematic representation of binding of ANS dye and Au nanoparticle to HSA protein.

located at subdomain IIA and IIIA in HSA.[11] Thus, Au nanoparticles can easily interact with the binding site at IA of HSA. Analysis of the results reveals that Au nanoparticle interacts with the binding site located at subdomain IA of HSA for all the three different-sized Au nanoparticles (shown in Figure 8). Thus, the surface energy transfer method is a convenient method to understand the interaction of protein−nanoparticles systems.

CONCLUSION

In summary, we have introduced three-body interactions among tryptophan of HSA, ANS-dye-labeled HSA protein, and Au nanoparticles to identify the location of Au nanoparticles in HSA protein. Here, ANS dye is used as a probe located at domain IIIA of HSA. Using surface energy transfer process, the distances from Trp residue to the probable binding site of HSA interacting with Au nanoparticles are obtained to be 42.5, 41.9, and 48.1 Å for 1.5, 2.0, and 2.9 nm HSA-conjugated Au nanoparticles, respectively. The measured distances between the binding site of ANS dye (located at domain IIIA) in HSA to the probable binding site of HSA interacting with Au nanoparticles are 51, 51.5, and 54.7 Å for 1.5, 2.0, and 2.9 nm HSA-conjugated Au nanoparticles, respectively. From the protein structural data (using PyMol software), the distances from the center of domain IIIA to Cys53−Cys62 disulfide bond and Trp to Cys53−Cys62 disulfide bond are obtained to be 51.5 and 39.1 Å, respectively. Thus, the distances calculated by using SET equation (Trp to Au binding site distance and ANS to Au binding site distance) nicely match the distances obtained from protein structural data by using PyMol software. It implies that the Au nanoparticles are attached to HSA by linkage with Cys53−Cys62 disulfide bond which is located at subdomain IA of HSA. Thus, we can say that Au nanoparticle interacts with the binding site located at subdomain IA of HSA for all the three different-sized Au-conjugated HSA systems. Therefore, such bioconjugated Au nanoparticles could pave the way for designing new optical-based materials for the application in chemical sensing or biological imaging.

ASSOCIATED CONTENT

Supporting Information. TEM images of the HSA-conjugated Au nanoparticles at pH 7.0 (Figure S1). Figure S2 shows the reverse phase chromatography profiles of pure HSA and Au nanoparticle conjugated HSA. Figure S3 shows anisotropy decay spectra of ANS in pure HSA and Au-conjugated HSA. This material is available free of charge via the Internet at http://pubs.acs.org.

AUTHOR INFORMATION

Corresponding Author

*E-mail: msap@iacs.res.in. Phone: (91)-33-2473-4971. Fax: (91)-33-2473-2805.

ACKNOWLEDGMENT

A.P. thanks to CSIR for generous funding. T.S., S.M., and S.H. thank CSIR for awarding fellowships.

REFERENCES

(1) Medintz, I. L.; Clapp, A. R.; Mattoussi, H.; Goldman, E. R.; Fisher, B.; Mauro, J. M. *Nat. Mater.* **2003**, *2*, 630–638.

(2) Michalet, X.; Pinaud, F. F.; Bentolila, L. A.; Tsay, J. M.; Doose, S.; Li, J. J.; Sundaresan, G.; Wu, A. M.; Gambhir, S. S.; Weiss, S. *Science (Washington, DC, U.S.)* **2005**, *307*, 538–544.

(3) Clapp, A. R.; Medintz, I. L.; Fisher, B. R.; Anderson, G. P.; Mattoussi, H. *J. Am. Chem. Soc.* **2005**, *127*, 1242–1250.

(4) Medintz, I. L.; Clapp, A. R.; Brunel, F. M.; Tiefenbrunn, T.; Uyeda, H. T.; Chang, E. L.; Deschamps, J. R.; Dawson, P. E.; Mattoussi, H. *Nat. Mater.* **2006**, *5*, 581–589.

(5) Clapp, A. R.; Medintz, I. L.; Mauro, J. M.; Fisher, B. R.; Bawendi, M. G.; Mattoussi, H. *J. Am. Chem. Soc.* **2004**, *126*, 301–310.
(6) Huang, X.; Li, L.; Qian, H.; Dong, C.; Ren, J. *Angew. Chem., Int. Ed.* **2006**, *45*, 5140–5143.
(7) Cedervall, T.; Lynch, I.; Lindman, S.; Berggard, T.; Thulin, E.; Nilsson, H.; Dawson, K. A.; Linse, S. *Proc. Natl. Acad. Sci. U.S.A.* **2007**, *104*, 2050–2055.
(8) Lynch, I.; Dawson Kenneth, A.; Linse, S. *Sci. STKE* **2006**, *2006*, e14.
(9) Lynch, I.; Dawson, K. A. *Nano Today* **2008**, *3*, 40–47.
(10) Klein, J. *Proc. Natl. Acad. Sci. U.S.A.* **2007**, *104*, 2029–2030.
(11) He, X. M.; Carter, D. C. *Nature* **1992**, *358*, 209–215.
(12) Carballal, S.; Radi, R.; Kirk, M. C.; Barnes, S.; Freeman, B. A.; Alvarez, B. *Biochemistry* **2003**, *42*, 9906–9914.
(13) Bagatolli, L. A.; Kivatinitz, S. C.; Aguilar, F.; Soto, M. A.; Sotomayor, P.; Fidelio, G. D. *J. Fluoresc.* **1996**, *6*, 33–40.
(14) Chi, Z.; Liu, R. *Biomacromolecules* **2011**, *12*, 203–209.
(15) Thumser, A. E. A.; Buckland, A. G.; Wilton, D. C. *J. Lipid Res.* **1998**, *39*, 1033–1038.
(16) Peters, T., Jr. *All About Albumin: Biochemistry, Genetics, and Medical Applications*; Academic Press: New York, 1995.
(17) Sudlow, G.; Birkett, D. J.; Wade, D. N. *Mol. Pharmacol.* **1975**, *11*, 824–832.
(18) De Paoli Lacerda, S. H.; Park, J.-J.; Meuse, C.; Pristinski, D.; Becker, M. L.; Karim, A.; Douglas, J. F. *ACS Nano* **2010**, *4*, 365–379.
(19) Loo, C.; Lowery, A.; Halas, N.; West, J.; Drezek, R. *Nano Lett.* **2005**, *5*, 709–711.
(20) Vallhov, H.; Qin, J.; Johansson, S. M.; Ahlborg, N.; Muhammed, M. A.; Scheynius, A.; Gabrielsson, S. *Nano Lett.* **2006**, *6*, 1682–1686.
(21) Gray, J. J. *Curr. Opin. Struct. Biol.* **2004**, *14*, 110–115.
(22) (a) Calzolai, L.; Franchini, F.; Gilliland, D.; Rossi, F. *Nano Lett.* **2010**, *10*, 3101–3105. (b) You, C.-C.; Verma, A.; Rotello, V. M. *Soft Matter* **2006**, *2*, 190–204.
(23) Jennings, T. L.; Singh, M. P.; Strouse, G. F. *J. Am. Chem. Soc.* **2006**, *128*, 5462–5467.
(24) Sen, T.; Sadhu, S.; Patra, A. *Appl. Phys. Lett.* **2007**, *91*, 043104−1–3.
(25) Persson, B. N. J.; Lang, N. D. *Phys. Rev. B* **1982**, *26*, 5409–5415.
(26) Sen, T.; Haldar, K. K.; Patra, A. *J. Phys. Chem. C* **2008**, *112*, 17945–17951.
(27) Sen, T.; Patra, A. *J. Phys. Chem. C* **2009**, *113*, 13125–13132.
(28) Sen, T.; Jana, S.; Koner, S.; Patra, A. *J. Phys. Chem. C* **2010**, *114*, 707–714.
(29) Lakowicz, J. R. *Principles of Fluorescence Spectroscopy*, 3rd ed.; Springer Publisher: New York, 2006.
(30) Giri, J.; Diallo, M. S.; Simpson, A. J.; Liu, Y.; Goddard, W. A.; Kumar, R.; Woods, G. C. *ACS Nano* **2011**, *5*, 3456–3468.
(31) Wangoo, N.; Suri, C. R.; Shekhawat, G. *Appl. Phys. Lett.* **2008**, *92*, 133104−1–3.
(32) Shang, L.; Wang, Y.; Jiang, J.; Dong, S. *Langmuir* **2007**, *23*, 2714–2721.
(33) Tayeh, N.; Rungassamy, T.; Albani, J. R. *J. Pharm. Biomed. Anal.* **2009**, *50*, 107–116.
(34) Rolinski Olaf, J.; Martin, A.; Birch David, J. S. *J. Biomed. Opt.* **2007**, *12*, 034013–1−7.
(35) Amiri, M.; Jankeje, K.; Albani, J. R. *J. Pharm. Biomed. Anal.* **2010**, *51*, 1097–1102.
(36) Flora, K.; Brennan, J. D.; Baker, G. A.; Doody, M. A.; Bright, F. V. *Biophys. J.* **1998**, *75*, 1084–1096.
(37) Zolese, G.; Falcioni, G.; Bertoli, E.; Galeazzi, R.; Wozniak, M.; Wypych, Z.; Gratton, E.; Ambrosini, A. *Proteins: Struct., Funct., Bioinf.* **2000**, *40*, 39–48.
(38) Amiri, M.; Jankeje, K.; Albani, J. R. *J. Fluoresc.* **2010**, *20*, 651–656.
(39) Suresh, D. V.; Mahesha, H. G.; Rao, A. G. A.; Srinivasan, K. *Biopolymers* **2007**, *86*, 265–275.
(40) Castellano, F. N.; Dattelbaum, J. D.; Lakowicz, J. R. *Anal. Biochem.* **1998**, *255*, 165–170.
(41) Ferrer, M. L.; Duchowicz, R.; Carrasco, B.; Garcia de la Torre, J.; Acuna, A. U. *Biophys. J.* **2001**, *80*, 2422–2430.
(42) Sahu, K.; Mondal, S. K.; Ghosh, S.; Roy, D.; Bhattacharyya, K. *J. Chem. Phys.* **2006**, *124*, 124909−1–7.
(43) (a) Matulis, D.; Baumann, C. G.; Bloomfield, V. A.; Lovrien, R. E. *Biopolymers* **1999**, *49*, 451–458. (b) Baker, G. A.; Pandey, S.; Kane, M. A.; Maloney, T. D.; Hartnett, A. M.; Bright, F. V. *Biopolymers* **2001**, *59*, 502–511. (c) Laptenok, S. P.; Visser, N. V.; Engel, R.; Westphal, A. H.; van Hoek, A.; van Mierlo, C. P. M.; van Stokkum, I. H. M.; van Amerongen, H.; Visser, A. J. W. G. *Biochemistry* **2011**, *50*, 3441–3450.
(44) Sen, T.; Haldar, K. K.; Patra, A. *J. Phys. Chem. C* **2010**, *114*, 11409–11413.